Efficient approximation of the Struve functions $\mathbf{H}_n$ occurring in the calculation of sound radiation quantities

Ronald M. Aarts[(a)] and Augustus J.E.M. Janssen[(b)]
[(a)]Philips Research Europe and
Department of Electrical Engineering, Eindhoven University of Technology
[(b)]Department of Mathematics and Computer Science,
TU-Eindhoven, MF 4.090, Den Dolech 2,
P.O. Box 513, 5600 MB Eindhoven
The Netherlands
email: ronald.m.aarts@philips.com

November 7, 2016

Abstract.
The Struve functions $\mathbf{H}_n(z)$, $n = 0, 1, \ldots$, are approximated in a simple, accurate form that is valid for all $z \geq 0$. In [R.M. Aarts, A.J.E.M. Janssen, J. Acoust. Soc. Am. **113**, 2635–2637 (2003)] the case $n = 1$, that arises in impedance calculations for the rigid-piston circular radiator mounted in an infinite planar baffle, has been done. The more general Struve functions occur when other acoustical quantities and/or non-rigid pistons are considered. The key step in the paper just quoted is to express $\mathbf{H}_1(z)$ as $\frac{2}{\pi} - J_0(z) + \frac{2}{\pi} I(z)$, where J_0 is the Bessel function of order zero and the first kind, and $I(z)$ is the Fourier cosine transform of $[(1-t)/(1+t)]^{1/2}$, $0 \leq t \leq 1$. The square-root function is optimally approximated by a linear function $\hat{c}t + \hat{d}$, $0 \leq t \leq 1$, and the resulting approximated Fourier integral is readily computed explicitly in terms of $\sin z/z$ and $(1 - \cos z)/z^2$. The same approach has been used

in [A. Maurel et al., Phys. Rev. B**75**, 224112 (2007)] to approximate $\mathbf{H}_0(z)$ for all $z \geq 0$. In the present paper, the square-root function is optimally approximated by a piecewise linear function consisting of two linear functions supported by $[0, \hat{t}_0]$ and $[\hat{t}_0, 1]$ with $\hat{t}_0$ the optimal take-over point. It is shown that the optimal two-piece linear function is actually continuous at the take-over point, causing a reduction of the additional complexity in the resulting approximations of $\mathbf{H}_0$ and $\mathbf{H}_1$. Furthermore, this allows analytic computation of the optimal two-piece linear function. By using the two-piece instead of the one-piece linear approximation, the RMS approximation error is reduced by roughly a factor of 3 while the maximum approximation error is reduced by a factor of 4.5 for $\mathbf{H}_0$ and of 2.6 for $\mathbf{H}_1$. Recursion relations satisfied by Struve functions, initialized with the approximations of $\mathbf{H}_0$ and $\mathbf{H}_1$, yield approximations for higher order Struve functions.

PACS number(s): 43.38.Ar, 43.20.Bi, 43.40.At

I Introduction

Struve functions are used in various disciplines of the applied sciences, such as optics, fluid dynamics, acoustics, aerodynamics, see [19], Subsec. 11.12 on p. 298 for a listing of applications. In [3], Sec. I, the role of the Struve function $\mathbf{H}_1$ in the computation of the impedance for the rigid-piston circular radiator mounted in an infinite baffle is reviewed. Struve functions $\mathbf{H}_n$ of order $n \neq 1$ occur in a number of cases where acoustical quantities for piston radiation are computed analytically. In [12], Subsecs. IV.B-C, Greenspan expresses the impedance for certain low-order non-rigid piston radiators in terms of $\mathbf{H}_0$, $\mathbf{H}_1$ and $\mathbf{H}_2$, and a similar thing is done in [12], Subsecs. V.B-C for the power output. The developments in [12] have been continued in [4] by Aarts and Janssen where Struve-type functions occur in a general setting for the calculation of impedance, power output as well as the edge pressure.

In [3], Sec. II an approximation of $\mathbf{H}_1(z)$ has been developed in terms of the Bessel function $J_0(z)$ and $\sin z/z$, $(1-\cos z)/z^2$ that is simple, accurate and valid for all $z \geq 0$ at the same time. Because of its accuracy and absence of patchwork for different z-regimes, this approximation has become quite popular among workers and teachers in and outside the acoustic community. The approximation in question reads

$$\mathbf{H}_1(z) \;=\; \frac{2z}{\pi} \int_0^1 \sqrt{1-t^2}\, \sin zt \, dt \tag{1a}$$

$$= \frac{2}{\pi} - J_0(z) + \frac{2}{\pi} \int_0^1 \sqrt{\frac{1-t}{1+t}} \cos zt \, dt \tag{1b}$$

$$\approx \frac{2}{\pi} - J_0(z) + \Big(\frac{16}{\pi} - 5\Big) \frac{\sin z}{z} + \Big(12 - \frac{36}{\pi}\Big) \frac{1 - \cos z}{z^2} \ , \tag{1c}$$

where the two equalities in (1a) and (1b) are exact, while the approximate identity in (1c) has been obtained by determining the least-mean-square fit $\hat{c} + \hat{d}t$ of $[(1-t)/(1+t)]^{1/2}$, $0 \le t \le 1$, and subsequently an explicit computation of the approximated integral $\int_0^1 (\hat{c} + \hat{d}t) \cos zt \, dt$. The squared approximation error in (1) on $[0, \infty)$ equals 2.2×10^{-4} while the maximum absolute error equals 0.0049.

The approximation in (1) is mentioned and used explicitly in [1], Eq. (18), [2], Eq. (9), [5], Eq. (37), [6], Eq. (7), [7], Eq. (9), [8], Eq. (37), [10], Eq. (4), [11], Eq. (A2), [13], Eq. (6), [14], Eq. (7), [15], Eq. (25), [16], Eq. (1.82) on p. 28, [17], Appendix C.2, [20], Eq. (7), [23], between Eqs. (25–26), and it is mentioned in passing in [4], below Eq. (29), [9], below Eq. (3), [24], above Eq. (10.52) on p. 464.

As said, the Struve function $\mathbf{H}_1(z)$ occurs in the analytical expression for the piston mechanical radiation impedance in the case of a rigid-piston radiator mounted in an infinite baffle, see [3] and [22], Sec. 5-4, pp. 221–225. In the same context, the pressure at the edge of the radiator is given by

$$\frac{p_{\text{edge}}}{\rho_0 c V_s} = \frac{1}{2}\Big[1 - J_0(2ka) + i\mathbf{H}_0(2ka)\Big], \tag{2}$$

where ρ_0 is the density of the medium, c is the speed of sound, $k = \omega/c$ is the wave number with ω the radial frequency of the vibrating piston, and V_s is the velocity of the piston, see [4], Sec. III and [21] pp. 163–164. Note the occurrence of the Struve function $\mathbf{H}_0(z)$ in (2).

In [17], Appendix C.2, there has been derived, using the method of [3], Sec. II, the approximation

$$\mathbf{H}_0(z) = \frac{2z}{\pi} \int_0^1 \frac{\sin zt}{\sqrt{1-t^2}} \, dt \tag{3a}$$

$$= J_1(z) + \frac{2}{\pi} \int_0^1 \sqrt{\frac{1-t}{1+t}} \sin zt \, dt \tag{3b}$$

$$\approx \quad J_1(z) + \Big(7 - \frac{20}{\pi}\Big)\,\frac{1-\cos z}{z} + \Big(\frac{36}{\pi} - 12\Big)\,\frac{\sin z - z\cos z}{z^2}\ . \quad (3c)$$

The maximum absolute error of this approximation equals 0.0056. Having available the approximation (1) and (3) for $\mathbf{H}_1(z)$ and $\mathbf{H}_0(z)$, one can approximate Struve functions $\mathbf{H}_n(z)$ of order $n = 2, 3, ...$ by using the recursive formula, see [19], 11.4.23 on p. 292

$$\mathbf{H}_{n+1}(z) = -\mathbf{H}_{n-1}(z) + \frac{2n}{z}\,\mathbf{H}_n(z) + \frac{(\frac{1}{2}\,z)^n}{\sqrt{\pi}\,\Gamma(n+\frac{3}{2})}\ , \qquad n = 1, 2, ...\ , \quad (4)$$

initialized by the approximations in (1) and (3).

Due to error propagation in the recursion (4), it is desirable to aim at high-accuracy approximations of $\mathbf{H}_0$ and $\mathbf{H}_1$. Increasing accuracy of the approximations is also beneficial for the investigations in [23], where considerable computer-time savings are reported when the approximation is used extensively, in [18], where (see above Eq. (6)) the approximation is used in the codes, and in [10], where the approximation in (1) is even declared to be an exact identity. It should be observed that infinite series expressions with excellent convergence behaviour exist for all $\mathbf{H}_n(z)$. For instance, see [19], 11.4.21 on p. 292,

$$\mathbf{H}_0(z) = \frac{4}{\pi}\sum_{k=0}^{\infty}\frac{J_{2k+1}(z)}{2k+1}\ . \quad (5)$$

Since $J_l(z)$ decays for fixed z very rapidly in l from $l = |z|$ onwards, it would be sufficient to include in the series in (5) all terms k with $2k+1 \geq \frac{3}{2}\,|z| + 5$, say, to have an excellent approximation to $\mathbf{H}_0(z)$. However, in this way, the truncation index becomes dependent on z, while the approximations in (1) and (3) have the appealing feature to have a fixed, and low, number of terms. The (known) result (5) is rediscovered in [6], Eq. (10).

In this paper, we improve the approximations in (1) and (3) by amplifying the approach used in [3], Sec. 2. Instead of a linear approximation $\hat{c} + \hat{d}t$ to the function $[(1-t)/(1+t)]^{1/2}$, we now use an approximation

$$\hat{f}(t) = \begin{cases} \hat{c}_1 + \hat{d}_1 t\ , & 0 \leq t < t_0\ , \\ \hat{c}_2 + \hat{d}_2 t\ , & t_0 < t \leq 1\ , \end{cases} \quad (6)$$

for this square-root function. Here $\hat{c}_1 = \hat{c}_1(t_0)$, $\hat{d}_1 = \hat{d}_1(t_0)$ and $\hat{c}_2 = \hat{c}_2(t_0)$, $\hat{d}_2 = \hat{d}_2(t_0)$ minimize, for a given t_0,

$$F_1(t_0\,;\,c,d) = \int_0^{t_0}\Big|\sqrt{\frac{1-t}{1+t}} - (c+dt)\Big|^2\,dt \quad (7)$$

and

$$F_2(t_0\,;\,c,d) = \int_{t_0}^{1} \left| \sqrt{\frac{1-t}{1+t}} - (c+dt) \right|^2 dt \ , \tag{8}$$

respectively, as a function of real c, d. Subsequently, we minimize the total mean square error

$$\begin{aligned} F(t_0) \ &= \ \int_{0}^{t_0} \left| \sqrt{\frac{1-t}{1+t}} - \hat{c}_1(t_0) - \hat{d}_1(t_0)\, t \right|^2 dt \\ &+ \ \int_{t_0}^{1} \left| \sqrt{\frac{1-t}{1+t}} - \hat{c}_2(t_0) - \hat{d}_2(t_0)\, t \right|^2 dt \end{aligned} \tag{9}$$

as a function of t_0. We have carried out the optimization of $F(t_0)$ numerically, and it turned out, surprisingly, that the resulting optimal $\hat{f}$ in (6) is continuous at $t = \hat{t}_0$, the optimal t_0. Hence, we have

$$\hat{c}_1(\hat{t}_0) + \hat{d}_1(\hat{t}_0)\, \hat{t}_0 = \hat{c}_2(\hat{t}_0) + \hat{d}_2(\hat{t}_0)\, \hat{t}_0 \ , \tag{10}$$

a fact that we have been able to establish mathematically. As a consequence, the optimal approximation can be computed completely analytically (except for numerically solving a simple and explicit equation for t_0). Furthermore, the additional complexity in approximating $\mathbf{H}_1(z)$ and $\mathbf{H}_0(z)$, when passing from an optimal linear approximation $\hat{c} + \hat{d}t$ to the optimal two-piece linear function $\hat{f}(t)$ in (6), is embodied by only one extra term

$$\frac{2}{\pi}\,(\hat{d}_2(\hat{t}_0) - \hat{d}_1(\hat{t}_0)) \cdot \begin{cases} \dfrac{1-\cos z t_0}{z^2} \\ \\ \dfrac{z t_0 - \sin z t_0}{z^2} \end{cases} \quad \text{and} \tag{11}$$

for (1) and (3), respectively.

In Sec. II we develop the optimal two-piece linear approximation to $[(1-t)/(1+t)]^{1/2}$, $0 \le t \le 1$, in detail. In Sec. III we compute the resulting approximations to $\mathbf{H}_1(z)$ and $\mathbf{H}_0(z)$, $z \ge 0$, taking advantage of continuity of the optimal piecewise linear approximations at the take-over point $\hat{t}_0$. In Sec. IV we give some considerations about approximation of $\mathbf{H}_n(z)$, $z \ge 0$, for $n = 2, 3, \ldots$, and in Sec. V we present our conclusions.

II Two-piece linear approximation of square-root function

A Best linear approximation on a single interval

We consider first a general, continuous, real-valued function f on the interval $[0,1]$ that is to be approximated as a linear combination of two continuous, real-valued functions g and h on a subinterval I of $[0,1]$. For real-valued functions k and l on I, we have the inner product and inner product norm

$$(k,l)_I = \int_I k(t)\, l(t)\, dt \ , \qquad \|k\|_I = \left(\int_I |k(t)|^2\, dt \right)^{1/2} \ . \tag{12}$$

When $I = [0,1]$, we delete the subscript I in (12).

It follows from elementary linear algebra for functions on an interval that the minimum of

$$\|f - (cg + dh)\|_I^2 \tag{13}$$

over all c and d is assumed for

$$c = \hat{c} = \frac{zv - yw}{xz - y^2} \ , \qquad d = \hat{d} = \frac{-yv + xw}{xz - y^2} \ , \tag{14}$$

where

$$x = x_I = (g,g)_I \ , \qquad y = y_I = (g,h)_I \ , \qquad z = z_I = (h,h)_I \ , \tag{15}$$

and

$$v = v_I = (f,g)_I \ , \qquad w = w_I = (f,h)_I \ . \tag{16}$$

Moreover,

$$(f - (\hat{c}g + \hat{d}h), g)_I = 0 = (f - (\hat{c}g + \hat{d}h), h)_I \ , \tag{17}$$

and the minimal mean square error is given by

$$\|f - (\hat{c}g + \hat{d}h)\|_I^2 = \|f\|_I^2 - \|\hat{c}g + \hat{d}h\|_I^2 = \|f\|_I^2 - (\hat{c}v + \hat{d}w) \ . \tag{18}$$

B Best approximation by two-component function

We next let $0 \le t_0 \le 1$, and we assume that we have continuous functions g_1 and h_1 on $[0,t_0]$ and g_2 and h_2 on $[t_0,1]$. We define $\hat{c}_1(t_0)$, $\hat{d}_1(t_0)$ and $\hat{c}_2(t_0)$, $\hat{d}_2(t_0)$ as the coefficients c_1, d_1 and c_2, d_2 for which

$$\|f - (c_1 g_1 + d_1 h_1)\|_{I=[0,t_0]}^2 \quad \text{and} \quad \|f - (c_2 g_2 + d_2 h_2)\|_{I=[t_0,1]}^2 \tag{19}$$

are minimal, respectively, with minimal values

$$F_1(t_0) = \int_0^{t_0} |f(t) - \hat{c}_1(t_0)\, g_1(t) - \hat{d}_1(t_0)\, h_1(t)|^2\, dt \tag{20}$$

and

$$F_2(t_0) = \int_{t_0}^{1} |f(t) - \hat{c}_2(t_0)\, g_2(t) - \hat{d}_2(t_0)\, h_2(t)|^2\, dt\ , \tag{21}$$

respectively. We intend to minimize

$$F(t_0) = F_1(t_0) + F_2(t_0) \tag{22}$$

over $t_0 \in [0, 1]$. It is shown in Appendix A (prime denoting differentiation with respect to t_0) that

$$\begin{aligned} F'(t_0) \;\; &= \;\; |f(t_0) - \hat{c}_1(t_0)\, g_1(t_0) - \hat{d}_1(t_0)\, h_1(t_0)|^2 \\ &\quad - |f(t_0) - \hat{c}_2(t_0)\, g_2(t_0) - \hat{d}_2(t_0)\, h_2(t_0)|^2\ . \end{aligned} \tag{23}$$

Hence, at any stationary point t_0 of F, we have

$$|f(t_0) - \hat{c}_1(t_0)\, g_1(t_0) - \hat{d}_1(t_0)\, h_1(t_0)| = |f(t_0) - \hat{c}_2(t_0)\, g_2(t_0) - \hat{d}_2(t_0)\, h_2(t_0)|\ . \tag{24}$$

In particular, when both quantities between the modulus signs in (24) have the same sign, we have

$$\hat{c}_1(t_0)\, g_1(t_0) + \hat{d}_1(t_0)\, h_1(t_0) = \hat{c}_2(t_0)\, g_2(t_0) + \hat{d}_2(t_0)\, h_2(t_0)\ . \tag{25}$$

That is, under this same-sign condition, the two-component function

$$\hat{f}(t) = \begin{cases} \hat{c}_1(t_0)\, g_2(t) + \hat{d}_1(t_0)\, h_1(t)\ , & 0 \le t < t_0\ , \\ \hat{c}_2(t_0)\, g_2(t) + \hat{d}_2(t_0)\, h_2(t)\ , & t_0 < t \le 1\ , \end{cases} \tag{26}$$

is continuous at any stationary point t_0 of f where the same-sign condition is valid.

C Specialization

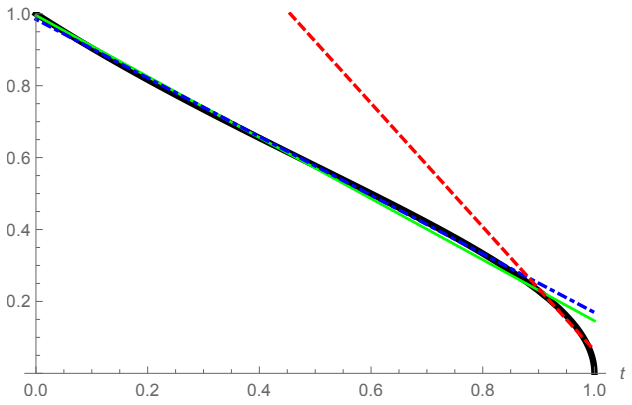

Figure 1: (Color online) The square root function $\sqrt{(1-t)/(1+t)}$ (solid bold line) vs. t. The optimal linear approximation (solid straight line). The optimal approximation on the interval $[0, \hat{t}_0]$ (dot-dashed line), and on the interval $[\hat{t}_0, 1]$ (dashed line), the latter two lines cross at $t = \hat{t}_0 = 0.883...$.

We consider now the case (see Fig. 1) that

$$f(t) = \sqrt{\frac{1-t}{1+t}}\,, \quad 0 \le t \le 1\ ; \qquad g_1(t) = 1\,, \quad h_1(t) = t\,, \quad 0 \le t \le t_0\ ,$$
$$g_2(t) = 1\,, \quad h_2(t) = t\,, \quad t_0 \le t \le 1\ . \tag{27}$$

We have now for (15) and (16)

$$x_1 = x_1(t_0) = t_0\,, \quad y_1 = y_1(t_0) = \tfrac{1}{2}\,t_0^2\,, \quad z_1 = z_1(t_0) = \tfrac{1}{3}\,t_0^3\ , \tag{28}$$

and

$$v_1 = v_1(t_0) = \Big[\sqrt{1-t^2} - 2\arctan\Big(\sqrt{\frac{1-t}{1+t}}\Big)\Big]_0^{t_0}\ , \tag{29}$$

$$w_1 = w_1(t_0) = \Big[(-1+\tfrac{1}{2}\,t)\,\sqrt{1-t^2} + \arctan\Big(\sqrt{\frac{1-t}{1+t}}\Big)\Big]_0^{t_0}\ . \tag{30}$$

The results (29), (30) can be verified directly by computing the derivatives of the right-hand sides as $[(1-t)/(1+t)]^{1/2}$ and $t\,[(1-t)/(1+t)]^{1/2}$, respectively. We compute from (14)

$$\hat{c}_1(t_0) + \hat{d}_1(t_0)\,t_0 = \frac{-2v_1(t_0)}{t_0} + \frac{6w_1(t_0)}{t_0^2}\ . \tag{31}$$

The computation of $\hat{c}_2(t_0) + \hat{d}_2(t_0)\, t_0$ can be done similarly, but is facilitated by considering $1 - t_0$, $f(1-t)$ in the above while noting that

$$\int_0^{1-t_0} f(1-t)\, dt = v_2(t_0)\ , \qquad \int_0^{1-t_0} t\, f(1-t)\, dt = v_2(t_0) - w_2(t_0)\ . \tag{32}$$

It is thus found that

$$\hat{c}_2(t_0) + \hat{d}_2(t_0)\, t_0 = \frac{-2v_2(t_0)}{1-t_0} + \frac{6(v_2(t_0) - w_2(t_0))}{(1-t_0)^2}\ . \tag{33}$$

It has been observed, by numerical inspection of the total error function F in (22) for the present case, that the optimal $t_0 = \hat{t}_0$ is to be found in the vicinity of 0.90. In this range, we have that $f(t_0) - \hat{c}_i(t_0) - \hat{d}_i(t_0)\, t_0$ is negative for both $i = 1$ and 2; also see Fig. 2.

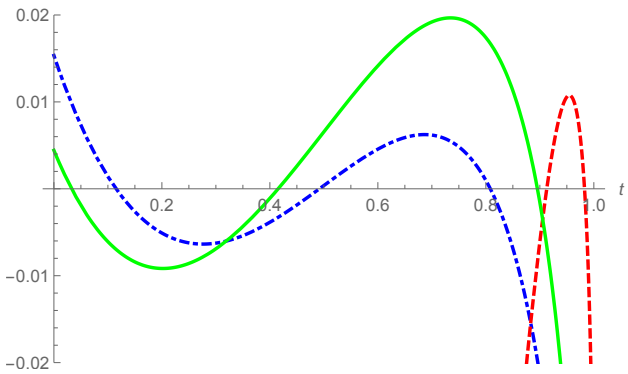

Figure 2: (Color online) The approximation errors vs. t corresponding to Fig. 1. The error of the approximation on the interval $[0, \hat{t}_0]$ (dot-dashed line) crosses the approximation error on the interval $[\hat{t}_0, 1]$ (dashed line) at $t = \hat{t}_0 = 0.883...$. The errors at $t = 1$ for the solid line and dashed line are equal to -0.146018366 and -0.063614711, respectively.

Hence, the same-sign condition is satisfied for the stationary point $\hat{t}_0$ near 0.90, and so $\hat{t}_0$ can be found by solving (25) for t_0 near 0.90. By (31) and (33), this becomes

$$\frac{-2v_1(t_0)}{t_0} + \frac{6w_1(t_0)}{t_0^2} = \frac{-2v_2(t_0)}{1-t_0} + \frac{6(v_2(t_0) - w_2(t_0))}{(1-t_0)^2}\ . \tag{34}$$

We eliminate $v_1(t_0)$ and $w_1(t_0)$ from (34) by using that

$$v_1(t_0) + v_2(t_0) = \int_0^1 \sqrt{\frac{1-t}{1+t}}\, dt = \frac{\pi}{2} - 1\ , \tag{35}$$

$$w_1(t_0) + w_2(t_0) = \int_0^1 t\,\sqrt{\frac{1-t}{1+t}}\,dt = 1 - \frac{\pi}{4}\ . \tag{36}$$

Furthermore, for $v_2(t_0)$ and $w_2(t_0)$ we have the explicit expressions (29) and (30) with limits t_0 and 1 rather than 0 and t_0. We then find after some further rearrangement the equation

$$\begin{aligned}&(6 - \tfrac{3}{2}\,\pi - (\pi - 2)\,t_0)(1 - t_0)^2 \\ &= \ (-6 + 8t_0 + 16t_0^2)\,\arctan\Big(\sqrt{\frac{1-t_0}{1+t_0}}\Big) + (6 - 12t_0 - 2t_0^2)\,\sqrt{1 - t_0^2}\ .\end{aligned} \tag{37}$$

It is found numerically that (37) holds for

$$t_0 = 0, 1, \text{ and } \hat{t}_0 = 0.8830472903...\ . \tag{38}$$

At $t_0 = \hat{t}_0$, we compute (using (14), (29–30), (35–36), (18) and the integral $\int \frac{1-t}{1+t}\,dt = 2\ln(1+t) - t$)

$$\hat{c}_1(\hat{t}_0) = 0.9846605676...\,, \quad \hat{d}_1(\hat{t}_0) = -0.8153693250...\ , \tag{39}$$

$$\hat{c}_2(\hat{t}_0) = 1.7825674761...\,, \quad \hat{d}_2(\hat{t}_0) = -1.7189527653...\ , \tag{40}$$

with residual mean square errors $F_1(\hat{t}_0)$ and $F_2(\hat{t}_0)$ given by 0.000026 and 0.000014, respectively. It is thus seen that the total residual mean square error $F(\hat{t}_0) = F_1(\hat{t}_0) + F_2(\hat{t}_0)$ is about 4×10^{-5}, which is a factor 8.5 lower than the residual mean square error 3.4×10^{-4} that was obtained in [3], Sec. 2 for the optimal linear function $\hat{c} + \hat{d}t$. The function $[(1-t)/(1+t)]^{1/2}$ with its optimal linear and optimal two-piece linear approximation is plotted in Fig. 1, and the corresponding approximation errors are plotted in Fig. 2.

With a glance at Fig. 1 and having in mind the accuracy gains just reported, increased complexity when breaking up the integration interval in more than two pieces is not likely to be compensated by significance of the further improved accuracy.

III Improved approximation of $\mathbf{H}_0$ and $\mathbf{H}_1$

We now compute the approximations of $\mathbf{H}_0(z)$ and $\mathbf{H}_1(z)$, $z \geq 0$, that follow by inserting the optimal two-piece linear function as an approximation of $[(1-t)/(1+t)]^{1/2}$ into the integrals in the third members in (1) and (3).

Thus, we let $\hat{f}(t)$ as in (6) with $t_0 = \hat{t}_0$ and $\hat{c}_1$, $\hat{d}_1$, $\hat{c}_2$, $\hat{d}_2$ given by (38) and (39–40). This $\hat{f}(t)$ is piecewise linear on $[0,1]$ and continuous at $t = \hat{t}_0$. For the integral in (1) we get, using partial integration,

$$\begin{aligned}
&\int_0^1 \sqrt{\frac{1-t}{1+t}}\,\cos zt\,dt \approx \int_0^1 \hat{f}(t)\cos zt\,dt \\
&= \frac{1}{z}\,\hat{f}(z)\sin zt\Big|_0^1 - \frac{1}{z}\int_0^1 \hat{f}'(z)\sin zt\,dt \\
&= (\hat{c}_2+\hat{d}_2)\,\frac{\sin z}{z} - \hat{d}_2\,\frac{1-\cos z}{z^2} + (\hat{d}_2-\hat{d}_1)\,\frac{1-\cos z\,\hat{t}_0}{z^2}\ . \qquad (41)
\end{aligned}$$

There results the approximation

$$\mathbf{H}_1(z) \approx \frac{2}{\pi} - J_0(z) + A_1\,\frac{\sin z}{z} + B_1\,\frac{1-\cos z}{z^2} + C_1\,\frac{1-\cos z\,\hat{t}_0}{z^2}\ , \qquad (42)$$

where

$$A_1 = \frac{2}{\pi}\,(\hat{c}_2+\hat{d}_2) = 0.0404983827...\ , \qquad (43)$$

$$B_1 = -\,\frac{2}{\pi}\,\hat{d}_2 = 1.0943193181...\ , \qquad (44)$$

$$C_1 = \frac{2}{\pi}\,(\hat{d}_2-\hat{d}_1) = -0.5752390840...\ , \qquad (45)$$

and $\hat{t}_0$ given in (38). The approximation in (42) for $\mathbf{H}_1(z)$ is of the same form as the one in (1), except for the last term.

In a similar fashion, we compute for the integral in (3)

$$\begin{aligned}
&\int_0^1 \sqrt{\frac{1-t}{1+t}}\,\sin zt\,dt \approx \int_0^1 \hat{f}(t)\sin zt\,dt \\
&= \frac{-1}{z}\,((\hat{c}_2+\hat{d}_2)\cos z - \hat{c}_1) + \hat{d}_1\,\frac{\sin z\,\hat{t}_0}{z^2} + \hat{d}_2\,\frac{\sin z - \sin z\,\hat{t}_0}{z^2} \\
&= \hat{c}_2\,\frac{1-\cos z}{z} + \hat{d}_2\,\frac{\sin z - z\cos z}{z^2} + (\hat{d}_2-\hat{d}_1)\,\frac{z\,\hat{t}_0 - \sin z\,\hat{t}_0}{z^2}\ , \qquad (46)
\end{aligned}$$

where in the last step we have used $\hat{c}_1 + \hat{d}_1\hat{t}_0 = \hat{c}_2 + \hat{d}_2\hat{t}_0$. There results the approximation

$$\mathbf{H}_0(z) \approx J_1(z) + A_0\,\frac{1-\cos z}{z} + B_0\,\frac{\sin z - z\cos z}{z^2} + C_0\,\frac{z\,\hat{t}_0 - \sin z\,\hat{t}_0}{z^2}\ , \qquad (47)$$

where

$$A_0 = \frac{2}{\pi}\,\hat{c}_2 = 1.134817700...\,, \quad B_0 = -B_1\,, \quad C_0 = C_1\,, \tag{48}$$

with B_1, C_1 given in (44), (45), and $\hat{t}_0$ given in (38).

In Fig. 3 we show the approximation errors associated to (42) and (47) as a function of z, $0 \le z \le 60$, where the exact results are obtained by using Mathematica (V.10). It is seen that the maximal absolute error for approximating $\mathbf{H}_1(z)$ is 0.00185 which is about a factor 2.6 lower than the maximal absolute error 0.00485 that can be obtained from Fig. 2 in [3] using the approximation (1). The maximal absolute approximation error in Fig. 3 is 0.00125 which is about a factor 4.5 lower than the maximal absolute error 0.00558 that can be obtained from Fig. 16 in [17].

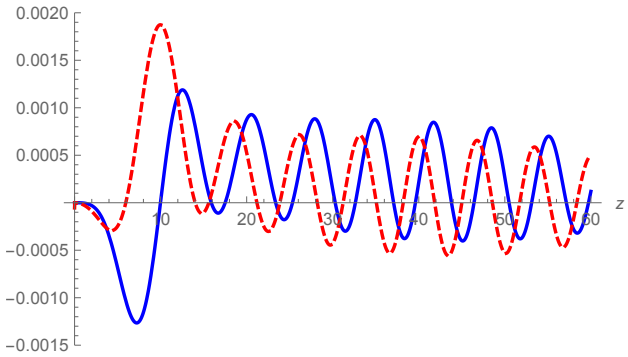

Figure 3: (Color online) The error in the approximation vs. z of $\mathbf{H}_0(z)$ (solid curve), by Eq. (47) and $\mathbf{H}_1(z)$ (dashed curve), by Eq. (42).

IV Approximation of $\mathbf{H}_n(z)$, $n = 2, 3, ...$

There are a number of conceivable approaches to approximate $\mathbf{H}_n(z)$, $n = 2, 3, ...$. We apply the approximation (42) and (47) for $\mathbf{H}_1(z)$ and $\mathbf{H}_0(z)$ to approximate Struve functions $\mathbf{H}_n(z)$ of order $n = 2, 3, ...$ by using the recursive formula (4). As an example we compute $\mathbf{H}_2(z)$ by this method and we show the result in Fig. 4.

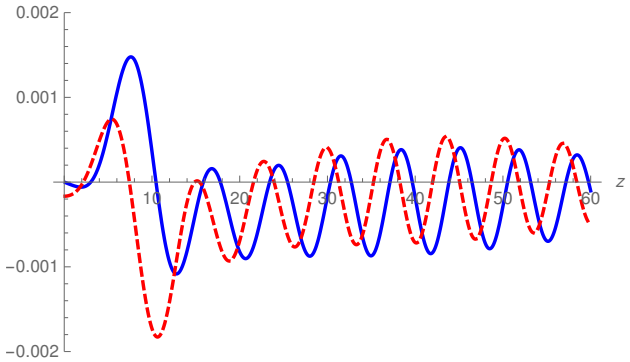

Figure 4: (Color online) The error in the approximation vs. z of $\mathbf{H}_2(z)$ (solid curve), and $\mathbf{H}_3(z)$ (dashed curve), using the approximations (42) and (47) and the recursive formula (4).

V Conclusions

Simple and effective approximations of the Struve functions $\mathbf{H}_0$ and $\mathbf{H}_1$ for all values of z have been developed using only a limited number of elementary functions. Using these approximations and a recursion formula, approximations for general order $\mathbf{H}_n$ can be computed. The obtained approximations have a higher accuracy than the one obtained in [17] for $\mathbf{H}_0$ and the one obtained in [3] for $\mathbf{H}_1$; the RMS approximation error is reduced by roughly a factor of 3 and the maximum approximation error is reduced by a factor of 4.5 for $\mathbf{H}_0$ and of 2.6 for $\mathbf{H}_1$, while the new approximations have each only one extra term. It does not require patchwork formulas, since it is accurate for the whole range of the independent variable z. The approximations can be used in various fields, with its most prominent engineering application in electroacoustics. The approximated $\mathbf{H}_1$ of [3] has been used in computer codes, see [18, 23]. The improved approximations are envisaged to extend the application range of methods and codes that require many evaluations of Struve functions at many points.

Appendix A: Proof of (23)

We have from basic calculus the formula

$$\frac{d}{dt_0}\left[\int_0^{t_0} G(t\,;\,t_0)\,dt\right] = G(t_0\,;\,t_0) + \int_0^{t_0} \frac{\partial G}{\partial t_0}(t\,;\,t_0)\,dt \qquad \text{(A1)}$$

when $G(t\,;\,t_0)$ is continuous in t and continuously differentiable in t_0. Using this with

$$G(t\,;\,t_0) = (f(t) - \hat{c}_1(t_0)\,g_1(t) - \hat{d}_1(t_0)\,h_1(t))^2\ , \tag{A2}$$

so that

$$\begin{aligned}\frac{\partial G}{\partial t_0}\,(t\,;\,t_0) \;&=\; -2(f(t) - \hat{c}_1(t_0)\,g_1(t) - \hat{d}_1(t_0)\,h_1(t)) \\ &\quad\cdot (\hat{c}_1'(t_0)\,g_1(t) + \hat{d}_1'(t_0)\,h_1(t))\ ,\end{aligned} \tag{A3}$$

and noting that $\hat{c}_1'(t_0)\,g_1(t) + \hat{d}_1'(t_0)\,h_1(t)$ is a linear combination of g_1 and h_1 on $I = [0, t_0]$, it follows from (17) that

$$\int_0^{t_0} \frac{\partial G}{\partial t_0}\,(t\,;\,t_0)\,dt = 0\ . \tag{A4}$$

Hence, see (20),

$$\begin{aligned}F_1'(t_0) &= \frac{d}{dt_0}\left[\int_0^{t_0} G(t\,;\,t_0)\,dt\right] \\ &=\; G(t_0\,;\,t_0) = |f(t_0) - \hat{c}_1(t_0)\,g_1(t_0) - \hat{d}_1(t_0)\,h_1(t_0)|^2\ .\end{aligned} \tag{A5}$$

Similarly, see (21),

$$F_2'(t_0) = -|f(t_0) - \hat{c}_2(t_0)\,g_2(t_0) - \hat{d}_2(t_0)\,h_2(t_0)|^2\ , \tag{A6}$$

and the proof of (23) is complete.

References

[1] R.M. Aarts, "High-efficiency low-Bl loudspeakers," J. Audio Eng. Soc. **53**, 579–592 (2005).

[2] R.M. Aarts, "Optimally sensitive and efficient compact loudspeakers," J. Acoust. Soc. Am. **119**, 890–896 (2006).

[3] R.M. Aarts and A.J.E.M. Janssen, "Approximation of the Struve function $\mathbf{H}_1$ occurring in impedance calculations," J. Acoust. Soc. Am. **113**, 2635–2637 (2003).

[4] R.M. Aarts and A.J.E.M. Janssen, "Sound radiation quantities arising from a resilient circular radiator," J. Acoust. Soc. Am. **126**, 1776–1787 (2009).

[5] E. Afsaneh and H. Yaveri, "Critical current of a granular d-wave superconductor," Solid State Comm. **152**, 1933–1938 (2012).

[6] A. Ahmadi, M.M. Abaiee, and M. Abbaspour, "Approximation of Struve function of zero order $\mathbf{H}_0$ occurring in hydrodynamics problems," presented at 5^{th} Offshore Industries Conference (OIC2013), 21–22 May 2013, Teheran.

[7] J. Ahonen, "Electroacoustic modelling of the subwoofer enclosures," Linearteam technical paper, 2007.

[8] M.R. Bai, B.-C. You, and Y.-Y. Lo, "Electroacoustic analysis, design and implementation of a small balanced armature speaker," J. Acoust. Soc. Am. **136**, 2554–2560 (2014).

[9] I. Djurek, D. Djurek, and A. Petošić, "Stochastic solutions of Navier-Stokes equations: An experimental evidence," Chaos **20**, 043107 (2010).

[10] I. Durek, M. Perković, and H. Domitrović, "On differences between a straight and curved transmission lines," presented at 5^{th} Congress of Alps-Adria, 12–14 September 2012, Petrčane, Croatia.

[11] M. Einhellinger, A. Cojuhovschi, and E. Jeckelmann, "Numerical method for nonlinear steady-state transport in one-dimensional correlated conductors," Phys. Rev. B**85**, 235141 (2012).

[12] M. Greenspan, "Piston radiator: Some extensions of the theory," J. Acoust. Soc. Am. **65**, 608–621 (1979).

[13] M. Inalpolat, M. Caliskan, and R. Singh, "Sound radiated by a resonant plate: comparative evaluation of experimental and computational methods," presented at NOISE-CON2008, 28–30 July 2008, Dearborn, Michigan.

[14] M. Inalpolat, M. Caliskan, and R. Singh, "Analysis of near field sound radiation from a resonant unbaffled plate using simplified analytical models," Noise Control Eng. J. **58**, 145–156 (2010).

[15] K. Jambrosic, B. Ivancevic, and A. Petosic, "Estimating ultrasound transducer parameters using KLM equivalent circuit model," presented at Forum Acusticum 2005, Budapest.

[16] E. Larsen and R.M. Aarts, *Audio Bandwidth Extension*, p. 22 (Wiley, Chichester, UK, 2004).

[17] A. Maurel, V. Pagneux, F. Barra, and F. Lund, "Interaction of a surface wave with a dislocation," Phys. Rev. B**75**, 224112 (2007).

[18] M. Moszynski and W. Lis, "A spice equivalent circuit for modeling the performance of dual frequency echo-sounder," Hydroacoustics **14**, 165–170 (2011).

[19] F.W.J. Olver, D.W. Lozier, R.F. Boisvert, and C.W. Clark, *NIST Handbook of Mathematical Functions*, Ch. 11, (Cambridge, New York, 2010).

[20] A. Petošić, M. Horvat, and B. Ivančević, "Estimating parameters of a silencer by solving Helmholtz equation using finite elements method," presented at Forum Acusticum 2005, Budapest.

[21] J.W.S. Rayleigh, *The theory of sound*, (Vol. 2, 1896, p. 162, Dover, reprinted 1945).

[22] A.D. Pierce, *Acoustics, An Introduction to Its Physical Principles and Applications*, p. 222 (ASA, New York, 1989).

[23] W.P. Rdzanek, W.J. Rdzanek, and D. Pieczonka, "The acoustic impedance of a vibrating annular piston located on a flat rigid baffle around a semi-infinite circular rigid cylinder," Archives of Acoustics **37**, 411–422 (2012).

[24] C.H. Sherman and J.L. Butler, *Transducers and Arrays for Underwater Sound*, 2nd ed., p. 538, (Springer, New York, 2007, 2016).

List of Figures